Measurement of the Polarized Structure Function $g_1^{\rm p}(x,Q^2)$ and the Polarized Gluon Distribution $\Delta g(x,Q^2)$ at HERA

A. Deshpande[a], V. W. Hughes[a], J. Lichtenstadt[b]
[a] Department of Physics, Yale University, New Haven, CT 06511, USA[1]
[b] School of Physics and Astronomy, The Raymond and Beverly Sackler Faculty of Exact Sciences, Tel Aviv University, Tel Aviv 69978, Israel [2]

Abstract

We present estimates of possible data on spin-dependent asymmetries in inclusive scattering of high energy polarized electrons by high energy polarized protons at HERA, including statistical errors, and discuss systematic uncertainties. We show that these data will provide important information on the low x behavior of the polarized structure function g_1 and will reduce the uncertainty in the determination of the first moment of the polarized gluon distribution $\Delta g(x,Q^2)$ from the QCD analysis of g_1 in NLO. Study of possible di-jet asymmetries observed at HERA using polarized beams has been shown to provide a direct measurement of $\Delta g(x,Q^2)$, which in conjunction with the NLO QCD analysis of g_1 will provide an accurate determination of $\Delta g(x,Q^2)$ and its first moment. We also consider the possibility of a $g_1^{\rm n}$ measurement using a polarized ^{3}He beam at HERA.

1 Introduction

Measurements of nucleon structure functions by lepton-nucleon inclusive electromagnetic scattering have been of fundamental importance in the study of the internal structure of the nucleon since its beginning and continuing to the present. The history of these experiments for both unpolarized and polarized scattering has shown that important new important new information has been obtained when measurements were extended to new kinematic regions. In the mid-1950's at Stanford, Hofstadter extended measurements of elastic electron-proton scattering to a higher Q^2 range of 1 $(\mathrm{GeV/c})^2$ and first observed that the proton has a finite size [1]. In the late 1960's at SLAC Friedman, Kendall and Taylor extended measurements of inelastic inclusive electron scattering to the deep inelastic region of $Q^2 > 1$ $(\mathrm{GeV/c})^2$ and discovered the parton substructure of the proton [2]. This substructure was further studied in muon nucleon deep inelastic scattering [3]. The extension of the data to lower x and higher Q^2 made possible by the HERA ep collider showed a surprisingly steep rise towards low x of the unpolarized structure function F_2 [4] whose explanation has led to an improved understanding of perturbative QCD.

Polarized DIS which determines the spin dependent structure function of the nucleon from measurements of spin dependent cross section asymmetries has a similar history. The subfield of polarized lepton-proton scattering was initiated in the period 1974-1983 with the Yale-SLAC

[1]Supported by the U.S. Department of Energy.
[2]Supported by the Israel Science Foundation of the Israeli Academy of Sciences.

E80 and E130 experiments [5] which determined the spin dependent structure function of the proton. These measurements extended down to $x = 0.1$ and were consistent with the predictions of the Ellis-Jaffe sum rule and of the Bjorken sum rule and with the naive quark-parton model view that the nucleon spin is carried by its constituent quarks. There then followed a similar experiment at CERN by the EM collaboration [6] which extended the kinematic range of the original SLAC measurements into the lower x range from $x = 0.1$ to 0.01. The results showed that the Ellis-Jaffe sum rule is violated, which implied that the quarks carry only a small fraction of the nucleon spin and that the strange sea in the nucleon is polarized.

This surprising result stimulated a large amount of experimental and theoretical work on the polarized structure functions. The next generation experiments by the SM Collaboration at CERN [7, 8] and by the SLAC Collaborations [9, 10] reduced significantly the statistical and the systematic uncertainties of the measurements and the kinematic range was extended to $x = 0.003$. In addition, spin structure functions for the deuteron and neutron as well as the proton were measured, thus providing the first experimental verification of the fundamental model-independent Bjorken sum rule. Furthermore these extensive data made possible a next-to-leading order QCD analysis of the Q^2 dependence of g_1, thereby providing a determination of the first moment of the polarized gluon distribution. Extensive theoretical work has been published in the last 10 years [11].

Nevertheless, polarized structure functions are still measured in a limited x and Q^2 range and a large uncertainty on the first moment of g_1 comes from the unknown behavior of g_1 at low x [8, 10]. The kinematic range accessible by the present day fixed target experiments is limited and therefore to obtain a significant extension of the kinematic range the scattering of polarized electrons by polarized protons must be studied in a collider mode at HERA. The polarized gluon distribution in a nucleon is still largely unknown. Complete next to leading order (NLO) QCD analysis of the Q^2 dependence of the present g_1 data have now been performed[12, 13, 14] They provided the first information on the first moment of the polarized gluon distribution. Such analyses suggest a fairly large contribution of the gluon to the spin of the nucleon, however with large uncertainties[8, 15]. It is therefore extremely important to consider measurements which will reduce the error on the polarized gluon distribution.

The HERA collider at DESY has 27.5 GeV electrons and 820 GeV protons. At present the proton beam at HERA is unpolarized whereas the electron/positron beam has a natural transverse polarization, which can be rotated into a longitudinal polarization in the interaction regions. Once the protons in the HERA ring are polarized it would be possible to measure polarization asymmetries and thus explore spin dependent structure functions in the full HERA kinematic range. The possible increase in the measured $x-Q^2$ range for spin structure function measurements is shown in Fig. 1. The scientific and technical problems involved in obtaining polarized protons in the HERA ring have been discussed in [16].

In this paper in Section 2 we review the current status of polarized parton distributions and in Section 3 we discuss measurements of g_1 at a polarized HERA collider and their impact on the knowledge the polarized structure functions and thereby on the polarized gluon distribution in the proton. We first show that the data from polarized colliding beam experiments at HERA would provide information on the low x behavior of g_1 and through QCD analysis of g_1 would substantially improve the determination of the first moment of the polarized gluon distribution. This part is an update of our work in the previous HERA workshop [17], but we now include in our analysis all new published data. It has been shown that analysis of di-jet asymmetries from polarized e-p collisions in HERA will provide a direct measurement of the

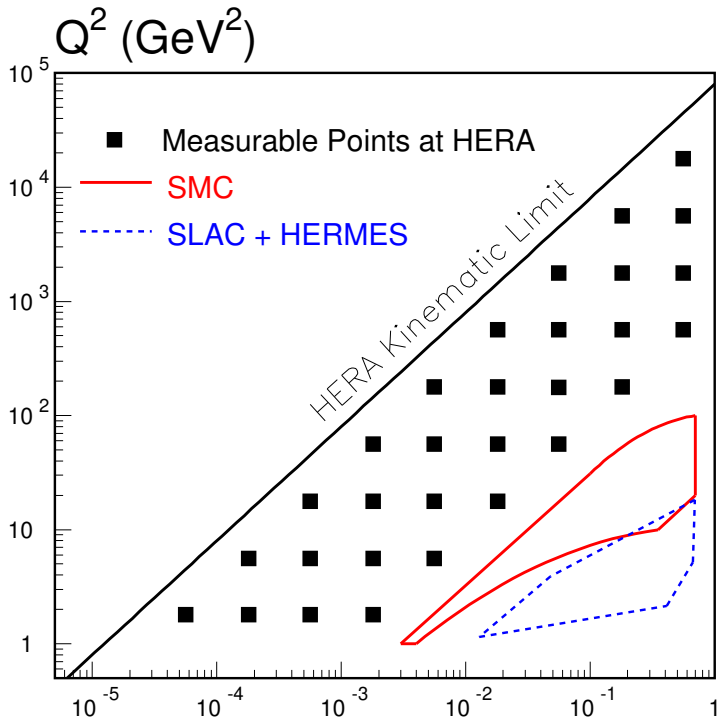

Figure 1: Measurable $x - Q^2$ region with polarized HERA shown with the presently explored regions by CERN(SMC), SLAC and DESY(HERMES) experiments, and the kinematic limit of measurability at HERA.

polarized gluon distribution [18]. We present for the first time (Section 4) an analysis which includes Δg measurements from di-jet asymmetries together with the QCD analysis of g_1 data from fixed target experiments and from HERA. The determination of the shape of the polarized gluon distribution $\Delta g(x, Q^2)$ and its first moment improves substantially from such a combined analysis. Lastly, in Section 5 we briefly comment on what one could learn about $g_1^{\rm n}$ if polarized ^{3}He can be stored in the HERA ring.

2 Current status of polarized parton distributions

The structure function g_1 is related to the polarized quark and gluon distributions through

$$\begin{aligned} g_1(x,t) &= \tfrac{1}{2}\langle e^2\rangle \int_x^1 \frac{{\rm d}y}{y}\Big[C_q^{\rm S}(\tfrac{x}{y},\alpha_s(t))\Delta\Sigma(y,t) \\ &+ 2n_f C_g(\tfrac{x}{y},\alpha_s(t))\Delta g(y,t) + C_q^{\rm NS}(\tfrac{x}{y},\alpha_s(t))\Delta q^{\rm NS}(y,t)\Big], \end{aligned} \tag{1}$$

where $\langle e^2\rangle = n_f^{-1}\sum_{k=1}^{n_f} e_k^2$, $t = \ln(Q^2/\Lambda^2)$, $\Delta\Sigma$ and $\Delta q^{\rm NS}$ are the singlet and non-singlet polarized quark distributions

$$\Delta\Sigma(x,t) = \sum_{i=1}^{n_f}\Delta q_i(x,t), \qquad \Delta q^{\rm NS}(x,t) = \sum_{i=1}^{n_f}(e_i^2/\langle e^2\rangle - 1)\Delta q_i(x,t),$$

and $C_q^{S,NS}(\alpha_s(Q^2))$ and $C_g(\alpha_s(Q^2))$ are the quark and gluon coefficient functions.

The x and Q^2 dependence of the polarized quark and gluon distributions is given by Altarelli-Parisi equations [19]. The full set of coefficient functions [20] and splitting functions [21] has been computed up to next to leading order in α_s. At next to leading order splitting functions, coefficient functions and parton distributions depend on renormalization and factorization scheme. The scheme choice is arbitrary and parton distributions in different factorization schemes are related to each other by well-defined linear transformations.

Polarized parton distributions can be obtained by fitting the experimental spin structure function data. In the analysis these distributions are parametrized at an initial scale and are evolved using the Altarelli-Parisi equations to values of x and Q^2 of the data, varying the parameters to fit the experimental values of g_1 [12, 13, 14]. Here we will follow the procedure used in refs. [12]. The initial parametrization at $Q^2 = 1$ GeV^2 has the form

$$\Delta f(x, Q^2) = N(\alpha_f, \beta_f, a_f)\ \eta_f\ x^{\alpha_f}(1-x)^{\beta_f}(1 + a_f\ x), \tag{2}$$

where $N(\alpha, \beta, a)$ is fixed by the normalization condition, $N(\alpha, \beta, a) \int_0^1 dx x^{\alpha}(1-x)^{\beta}(1+ax) = 1$, and Δf denotes $\Delta\Sigma$, Δq_{NS}, or Δg. With this normalization the parameters η_g, η_{NS}, and η_Σ are the first moments of the polarized gluon distribution, the non-singlet quark distribution (in proton or in the neutron), and the singlet quark distribution, respectively, at the initial scale. In this parametrization α_f and β_f determine the low x and high x behavior of the parton distribution, respectively, and the polynomial describes its mid-x region. Some variations of the initial parton distributions were also tried in order to check the dependence of the results on the choice of the parameterization. The evolution was performed within the AB factorization scheme (which has $C_g^1 = -\frac{\alpha_s}{4\pi}$). Further theoretical details of the fit procedure and analysis can be found in refs. [12, 15]. Following this scheme, the SM Collaboration performed a QCD analysis in NLO to existing polarized structure function data for proton, neutron and deuteron measured at SLAC, CERN and DESY [6, 7, 8, 9, 10, 22]. The results for the best fit coefficients are shown in Table 1 column 2. The fit to the world's proton data is shown in Fig. 2. The first moment of the gluon distribution resulting from this fit is: $\eta_g = 0.9 \pm 0.3(\text{exp}) \pm 1.0(\text{theory})$ at $Q^2 = 1$ GeV^2. Similar results were obtained by an analysis performed by Altarelli et al. [15]. The experimental error depends on the statistical and systematic uncertainty in the measured data points, while the theoretical uncertainty comes mainly from the choice of the factorization and renormalization scales, the initial parton distribution and the uncertainty in the value of α_s. The fit is determined mostly from the observed scaling violations in the intermediate and low x region. Clearly the uncertainty on the size of the polarized gluon distribution is large. The existing data poorly constrain the low x behavior of the various parton distributions and hence the values of α_Σ, α_g, and α_{NS}. Moreover, it is observed [15] that very different functional forms for the initial parton distributions give different predictions for the low x asymptotic behavior of $g_1(x)$ and also the values of the first moment of the polarized parton distribution, although the quality of the fit remains practically the same.

The behavior of g_1 at low x is still not determined. Indeed, unpolarized structure function data measured at HERA showed that F_2 rises at low x as predicted by pQCD [23], and does not follow a Regge behavior. The extrapolation of g_1 from the measured region down to $x = 0$, required to obtain it first moment, has been done so far assuming Regge behavior of the structure function, which implies [24] $g_1 \sim x^\alpha$ as $x \to 0$ with $0 \leq \alpha \leq 0.5$, i.e. a valence-like behavior of g_1. This behavior disagrees with that predicted by the QCD analysis[8] as is shown in Fig. 3. An experimental measurement of the low x behavior of g_1 would thus lead to significant insight on the structure of QCD both within and beyond perturbation theory.

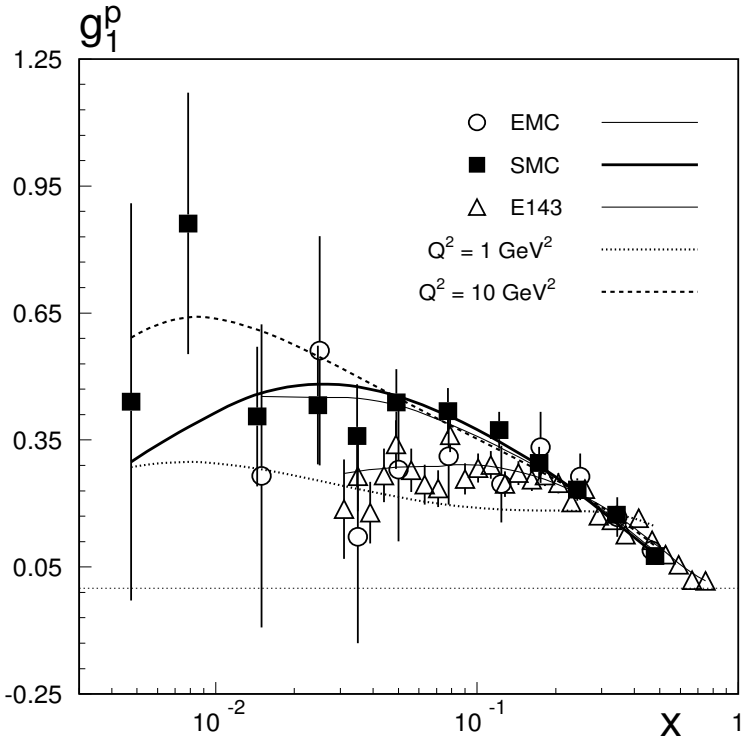

Figure 2: The NLO fit to proton $g_1^{\rm p}$ data. The solid lines are fits to data at the measured Q^2 values, and the dashed and the dotted lines are fits evolved to $Q^2 = 1$ and 10 GeV^2 respectively.

The low x information for the polarized case is crucial to obtain a good determination of the moments of g_1 [8, 10], since they include a contribution from an extrapolation into the unmeasured region.

3 Measurement of $g_1^{\rm p}(x, Q^2)$ at HERA and its impact

Presently all measurements of polarized structure functions are made by deep inelastic lepton-nucleon scattering on fixed targets. Figure 1 shows the kinematic ranges in which polarized lepton-proton data have been obtained at SLAC and CERN as well as the large extension in the $x - Q^2$ range which can be achieved at HERA with 820 and 27.5 GeV polarized proton and electron beams, respectively. A detailed study of a possible measurement of g_1 at HERA has been performed, assuming an integrated luminosity of $\mathcal{L} = 500$ pb^{-1} and electron and proton polarizations of 0.7. Kinematic cuts were applied based on the standard cuts made for analysis of data from the present HERA detectors: 1) The angle of the scattered electron θ'_e is required to be $< 177°$, 2) the inelasticity y is limited to $0.01 < y < 0.9$, 3) Consider data with $Q^2 > 1$ GeV^2 and 4) The energy of the scattered electron E'_e was required to be > 5 GeV. Results for the expected number of events for different (x, Q^2) bins are listed in Table 1, together with the average y and depolarization factor $D = (y(2-y))/(y^2 + 2(1-y)(1+R))$, and the measured asymmetry δA_m. Standard deep inelastic scattering formulae [17, 25] were used to calculate the kinematics and statistical uncertainties on the measured asymmetries. Using the best-fit parton distributions obtained from the QCD analysis of the data discussed in Sect. 2 predictions were made from the evolution equations for $g_1(x, Q^2)$ values and hence for cross

Parameter	Published results	HERA $\mathcal{L} = 500$ pb^{-1}
η_g	0.86±0.25	0.89 ± 0.15
η_q	0.40±0.04	0.38 ± 0.03
$\eta_{NS}^{\mathrm{p,n}}$	Fixed	Fixed
α_g	-0.47±0.25	-0.59± 0.13
α_q	0.73±0.30	0.87 ± 0.28
α_{NS}^{p}	-0.10±0.10	-0.13±0.09
α_{NS}^{n}	-0.10±0.16	0.06± 0.16
β_g	4.0(fixed)	4.0(fixed)
β_q	1.30±0.73	1.48±0.68
β_{NS}^{p}	1.48±0.28	1.39±0.26
β_{NS}^{n}	2.56±0.60	2.62± 0.59
a_q	-1.4±0.09	-1.4± 0.08
a_{NS}^{p}	0.0(fixed)	0.0(fixed)
a_{NS}^{n}	0.0(fixed)	0.0(fixed)

Table 1: Results of the QCD analysis in NLO. Results from the fit to all available published data. The parameters $\eta_{NS}^{\mathrm{p,n}}$ are fixed by the octet hyperon β decay constant. The parameter η_g stands for the first moment of the gluon distribution. All values of the parameters are given at $Q^2 = 1$ GeV^2.

section asymmetries in the HERA range. The systematic uncertainties in these measurements will be discussed in Sect. 3.1.

As shown in Fig. 1, measurements of g_1 at HERA will extend the x region down to $x = 5.6 \times 10^{-5}$. In Fig. 3 we show the expected accuracy of the determination of g_1 at HERA within the maximal extent of variation in the low x behavior compatible with the requirement of integrability of g_1 (which implies that at small x g_1 can rise at most as $1/(x \ln^{\alpha} x)$ with $\alpha > 1$). The figure also shows that a polarized HERA can clearly distinguish between the different prescriptions for the g_1^{p} behaviors in the low x region.

The full coverage of HERA experiments is shown in Figs. 3 and 4 where projected data with their estimated errors, assuming an integrated luminosity of $\mathcal{L} = 500$ pb^{-1} and beam polarizations of $P_p = P_e = 0.7$, are given on the basis of the NLO fit of Table 2. We consider two cases: a) the first moment of the gluon distributions is fixed to be 0 at Q^2 = 1 GeV^2 (minimal gluon: dashed lines in Fig. 4 a) and b) the first moment of the singlet quark density was fixed to $\eta_q = a_8$ at the same reference scale (maximal gluon: dotted lines in Fig.4). Of course yet wider deviations from these fits are possible since the low x behavior of the current best fit is only very loosely constrained due to the lack of direct experimental information at low x; also higher order corrections beyond NLO may turn out to be important at very low x. In Fig. 4 we show the statistical errors for each measurable data point in the complete $x - Q^2$ grid indicated in Fig. 1 and in Table 2. The bold solid lines are the predictions of g_1 values in the HERA kinematic range using the best fit parameters from the NLO-QCD analysis of all present-day data [7, 8, 9, 10]. The gluon distribution is only determined by the scaling violations of g_1. Therefore a reasonably wide kinematic coverage is required in order to achieve such a determination with satisfactory accuracy: in particular, since the gluon distribution is peaked at low x, data in this region with a large span in Q^2, such as those obtainable at HERA, would substantially improve the determination of $\Delta g(x, Q^2)$.

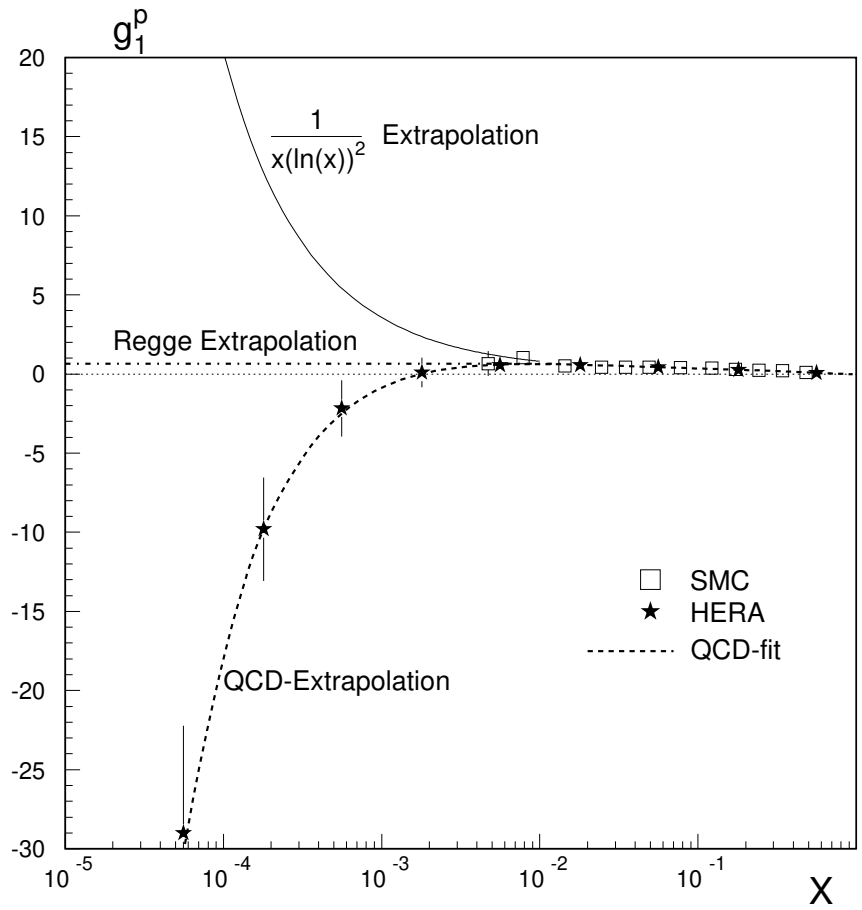

Figure 3: The statistical uncertainty on structure function g_1^{p} measurable at HERA for $Q^2 = 10\mathrm{GeV}^2$ with integrated luminosity $L = 500\ \mathrm{pb}^{-1}$ is shown. The SMC measurements are shown for comparison. Starting from the measured values of g_1^{p} by SMC, the possible values for g_1^{p} at low-x are shown in three plausible cases: valence-like Regge behavior $g_1(x) \sim x^{-\alpha}$ with $\alpha = 0$ or strong powerlike positive rise $g_1(x) \sim \pm 1/(x \cdot (\ln x)^2)$, and the pQCD prediction based on present best fit.

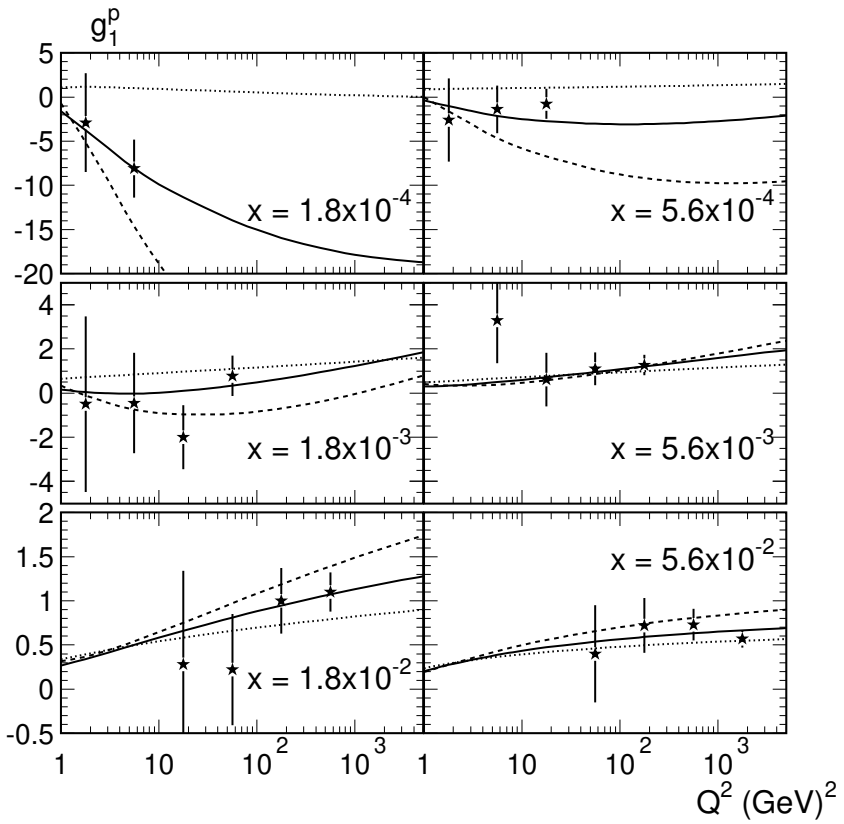

Figure 4: Predicted values for g_p^1 from NLO fits together with estimated statistical uncertainties for a future polarized DIS experiment with an integrated luminosity L=500 pb^{-1}. The solid bold lines are predictions based on fits to SMC and SLAC data extended in to the HERA kinematic range while the dotted and dashed lines are the maximal and minimal gluon predictions (see text).

x	Q^2 GeV^2	y	D	N_{total}	δA_m
5.6×10^{-5}	1.8	0.40	0.47	3.8×10^6	5.1×10^{-4}
1.8×10^{-4}	1.8	0.13	0.13	6.9×10^6	3.8×10^{-4}
	5.6	0.40	0.46	2.8×10^6	6.0×10^{-4}
5.6×10^{-4}	1.8	0.04	0.04	1.0×10^7	3.1×10^{-4}
	5.6	0.13	0.13	4.9×10^6	4.5×10^{-4}
	1.8×10^1	0.40	0.47	1.4×10^6	8.6×10^{-4}
1.8×10^{-3}	1.8	0.01	0.01	1.4×10^7	2.7×10^{-4}
	5.6	0.04	0.04	7.3×10^6	3.7×10^{-4}
	1.8×10^1	0.13	0.13	2.4×10^6	6.4×10^{-4}
	5.6×10^1	0.40	0.47	6.9×10^5	1.2×10^{-3}
5.6×10^{-3}	5.6	0.01	0.01	9.2×10^6	3.3×10^{-4}
	1.8×10^1	0.04	0.04	3.6×10^6	5.3×10^{-4}
	5.6×10^1	0.13	0.13	1.2×10^6	9.3×10^{-4}
	1.8×10^2	0.40	0.47	3.1×10^5	1.8×10^{-3}
1.8×10^{-2}	1.8×10^1	0.01	0.01	4.1×10^6	4.9×10^{-4}
	5.6×10^1	0.04	0.04	1.5×10^6	8.3×10^{-4}
	1.8×10^2	0.12	0.13	5.1×10^5	1.4×10^{-3}
	5.6×10^2	0.40	0.47	1.3×10^5	2.8×10^{-3}
5.6×10^{-2}	5.6×10^1	0.01	0.01	1.4×10^6	8.5×10^{-4}
	1.8×10^2	0.04	0.04	4.4×10^5	1.5×10^{-3}
	5.6×10^2	0.12	0.13	1.4×10^5	2.7×10^{-3}
	1.8×10^3	0.40	0.47	3.7×10^4	5.2×10^{-3}
1.8×10^{-1}	1.8×10^2	0.01	0.01	3.1×10^5	1.8×10^{-3}
	5.6×10^2	0.04	0.04	9.8×10^4	3.2×10^{-3}
	1.8×10^3	0.13	0.13	2.8×10^4	6.0×10^{-3}
	5.6×10^3	0.40	0.47	6.9×10^3	1.2×10^{-2}
5.6×10^{-1}	5.6×10^2	0.01	0.01	1.4×10^4	8.4×10^{-3}
	1.8×10^3	0.04	0.04	3.9×10^3	1.6×10^{-2}
	5.6×10^3	0.13	0.13	9.8×10^2	3.2×10^{-2}
	1.8×10^4	0.40	0.47	2.1×10^2	6.9×10^{-2}

Table 2: The kinematic variables x, Q^2, y, and D, along with the number of events expected $N_{\rm total}$, and the statistical uncertainty in the measured asymmetry $\delta A_{\rm m}$ in the kinematical region assuming an integrated luminosity L =500 pb^{-1} and proton and electron beam polarizations $P_{\rm p} = P_{\rm e} = 0.7$.

To assess the impact of these data we have repeated the QCD analysis described in section 2 with the addition of the projected HERA data. The values of g_1 predicted by the QCD analysis today were randomized within the statistical errors estimated for such measurements and assuming a Gaussian distribution of these values. The values of the best-fit parameters (Table 1 column 3) of course remain the same within the error, but using the estimated errors from acceptance considerations on measurable g_1, we get an estimate of the extent of reduction in the measured uncertainties of various parameters. In table 1 we show the results of fits with HERA data for integrated luminosities of $\mathcal{L} = 500$ pb^{-1}. Note in particular the sizable improvement in the determination of the first moment of Δg, which is of greatest theoretical interest due to its role in the understanding of the proton spin structure [11]: from $\delta(\eta_g) = \pm 0.3$ (the present value) to ± 0.2 for the above mentioned luminosity at HERA.

3.1 Systematic errors for HERA data

Normalization errors and false asymmetries constitute the principal sources of systematic errors associated with spin dependent asymmetry measurements. The normalization errors include principally uncertainties in the electron polarization P_e and in the proton polarization P_p . These lead to a change in the magnitude of the measured asymmetry by an amount which is small compared to the statistical error, and hence they are important primarily when evaluating the first moment of $g_1^{\mathrm{p}}(x)$.

Electron polarization P_e measurements by Compton scattering from polarized laser light have achieved [22] a relative uncertainty of 5%, and plans are being implemented to improve the accuracy by a factor of 2.

Absolute measurement of the polarization of the high energy (800 GeV) proton beam presents a new challenge and is presently under investigation at RHIC and at HERA. Several methods are being considered:

1. $\mathrm{p} - \vec{\mathrm{p}}$ elastic scattering in the Coulomb-nuclear interference region[26],
2. Inclusive π^+ or π^- production in collisions of 820 GeV protons with a fixed proton target
3. $\mathrm{p} - \vec{\mathrm{p}}$ scattering using a stationary polarized proton jet target and comparing for some scattering process the asymmetries $A_{\mathrm{beam}} = A_{\mathrm{jet}}$, where A_{beam} is the asymmetry in the scattering of the polarized beam from an *unpolarized* jet and A_{jet} is the asymmetry measured with an *unpolarized* beam and a polarized jet target with a known polarization P_{jet}. Adjusting the jet polarization to obtain the same asymmetry $A_{\mathrm{beam}} = A_{\mathrm{jet}}$, one obtains the beam polarization $P_{\mathrm{beam}} = P_{\mathrm{jet}}$ [27].

We comment briefly on these possible methods. For method 1 the nuclear matrix element may not be known well enough to provide a significant absolute determination of P_{p}. Method 2 appears to be a simple method for a relative measurement of the polarization [28]. Method 3 appears quite attractive because only an invariance principle is needed from theory, and it may be possible to use the stationary polarized target of the HERMES experiment for this measurement. It is reasonable to expect that a 5% accuracy can be achieved. Methods to measure P_{p} are presently considered and studied also for polarized protons at RHIC. Detailed discussions of the various options are given in to [29, 30, 31, 32]

The other type of systematic error comes from false asymmetries. These arise from variations in counting rate due to time variations in detector efficiencies, beam intensities, or crossing angles between the conditions of spins parallel and antiparallel. In view of the expected small values of the true asymmetries expected in the HERA kinematic region, (Table 2), the false asymmetries must be controlled at the level of 10^{-4}. We note that medium and high energy experiments which have measured parity violation have controlled false asymmetries to less than 10^{-5} to 10^{-8} [33].

False asymmetries can be avoided by frequent reversals of spin orientations. In the HERA collider the electron(positron) spin reversal is difficult and time consuming (several hours) and would lead to changes in beam intensity and beam emittance. Hence asymmetry data must be obtained with a fixed helicity for the electron beam by varying the proton helicity. Both the electron and proton rings are filled with about 200 particle bunches. The proton ring can be filled with bunches of protons with individually predetermined polarizations. Parallel and antiparallel spin data would be obtained at successive beam crossings occurring at time intervals of about 100 ns. Such alternations eliminate many errors in an asymmetry measurement. However, differences in the intensities and the crossing angles at successive proton bunches could still lead to false asymmetries and will have to be minimized.

The most important approach to avoid false asymmetries will be to use a spin rotator to reverse the helicity of all proton bunches at adequately frequent intervals (perhaps once per 8 hours). The design of such rotators has been studied and appears practical without appreciable change in the orbits, or in the magnitude of proton polarization [34]. Studies at the IUCF at 370 MeV have confirmed these conclusions [35]. In addition to this, shifting of proton beam bunches by about 100 ns by increasing or decreasing the orbit length by the appropriate amount could also effectively change the orientation of colliding beam bunches. This would create the same effect created by the spin rotator, and is expected to be possible every second. Combining these approaches the false asymmetries could be controlled to less than 10^{-4}.

4 Combined QCD analysis of g_1 data and Δg from di-jet asymmetries

QCD analysis of spin structure function data determines the first moment of the polarized gluon distribution in the nucleon. From the discussion in Sect. 2 and 3, although the statistical uncertainty in the measurement of Δg would be significantly reduced from a pQCD analysis of the HERA data along with the presently available data, theoretical uncertainties still remain large. By increasing the range in $x - Q^2$ surely some of them reduce. It is evident that contrary to the situation of the unpolarized gluon distribution measurement, the polarized gluon distribution Δg will be constrained less severely by the Q^2 dependence of g_1. The statistical errors will be much larger, primarily due to the depolarization factor that dilutes the polarized measurements compared to those in the unpolarized case. Effectively, this makes the determination of the scaling violations less precise. Therefore it is worth exploring the possibilities of other measurements which are sensitive to Δg.

It has been shown by H1 at HERA [36] that the unpolarized gluon momentum distribution $g(x)$ can be accessed in a direct way by measuring the cross section of di-jet production in DIS. The processes which contribute to the di-jet cross section are photon gluon fusion (PGF) and

Data used	$\delta(\int \Delta g)$
QCD Anal. of published g_1 today (= "A")	± 0.3
"A" + Projected HERA g_1^p	± 0.2
"A" + Projected HERA Δg-jets	± 0.2
"A" + Projected HERA g_1^p and Δg-jets	± 0.1

Table 3: The expected uncertainty in the determination of the first moment of the gluon distribution at $Q^2 = 1$ GeV^2 with possible inclusive and di-jet data available from polarized HERA with $\mathcal{L} = 500$ pb^{-1}.

QCD Compton scattering (QCDC). Measurement of the asymmetry in di-jet production will thus provide a direct measurement of the polarized gluon distribution $\Delta g(x)$. Simulations of di-jet asymmetries and details of the analysis to obtain the polarized gluon distribution are discussed in [18]. It is thus interesting to study the impact of a combined analysis of g_1 and Δg values obtained from such di-jet asymmetry data on the determination of Δg. In this section we use the projected data from polarized di-jets and show that when used along with the QCD analysis of g_1 the uncertainties on the first moment of the polarized gluon are reduced and the low x behavior of g_1 is constrained.

In principle, such analysis should be carried out using the measured di-jet asymmetries and g_1 data in a self consistent procedure in NLO. Polarized parton and gluon densities should be fitted simultaneously to both data sets, to reproduce the scaling violations in g_1 and separate the PGF and QCDC contributions[18] to the jet asymmetry cross sections. The tools to perform such analysis are not available yet. However, the effect of the combined analysis on the uncertainty in Δg can be assessed by including the values of Δg obtained from the di-jet analysis in the NLO QCD fit of the g_1 data as an extra constraint.

The values $\Delta g(x)$ obtained from the best fit of present-day g_1 data, evolved to $Q^2 = 20$GeV^2 were considered then as data which would be extracted from the analysis of the di-jet asymmetries with statistical errors obtained from the MC simulation discussed in [18], for an integrated luminosity of 500 pb^{-1}. Di-jet events used in this analysis were selected using the following criteria: 1) $E_T > 5$ GeV for both jets, 2) 5 GeV^2 $< Q^2 <$ 100 GeV^2, 3) $0.3 < y < 0.85$, and 4) $\hat{s} > 100$GeV^2. Like the projected g_1 data for the HERA kinematic region, they were randomized around the calculated value within one standard deviation of the statistical error. As mentioned in Section 3, including the projected g_1 data in the NLO analysis reduced the error on the first moment of Δg by about 30%, yielding $\eta_g = 0.9 \pm 0.2$, down from $\delta(\eta_g) = 0.3$. The QCD analysis of the actual data as well as the projected g_1 data was repeated including also he Δg values as part of the χ^2-test. While the best fit parameters are obviously about

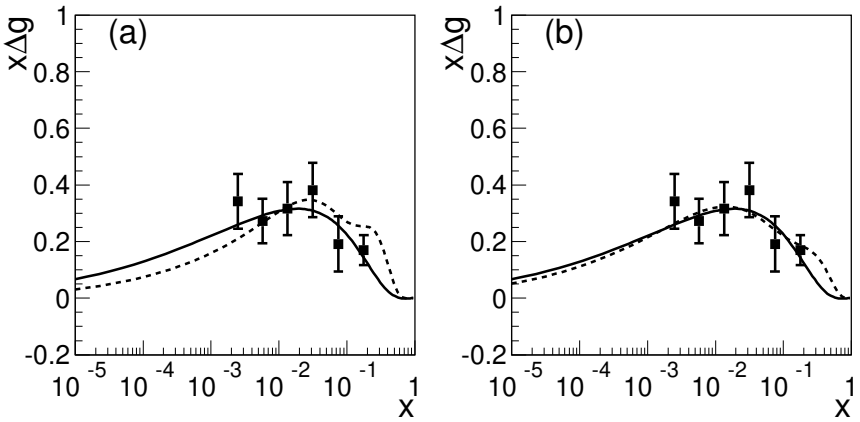

Figure 5: (a) Comparison of polarized gluon distribtions at $Q^2 = 20$ GeV^2 obtained with a 14 parameter fit (Eq. 3) with those obtained from a 10 parameter fit (Eq. 2). (a) - Results of 14 parameter fit of present data data (dashed line) and 10 parameter fit of data and projected data. (b) Results of 14 parameter and 10-parameter fits of data and projected data. Also shown are projected $\Delta g(x)$ values with their statistical errors from di-jet asymmetries, obtained from a 10 parameter fit.

the same as those obtained for the NLO fit of the g_1 data, the uncertainty on the first moment of the polarized gluon distribution is reduced by 50%, yielding $\eta_g = 1.0 \pm 0.1$. The polarized gluon distribution from the best fit of g_1 data, and projected HERA data, evolved to 20 GeV^2 is shown in Fig.5 along with the $pseudo - data$ of Δg used in the fit. The effect of the di-jet data alone on the uncertainty in η_g is similar to that of adding to the presently available data, only the projected g_1 data which will be measured at HERA. The combined fit of present-day g_1 data with the Δg from di-jet asymmetries yields $\eta_g = 1.0 \pm 0.2$. The results for the first moments of the polarized gluon distributions obtained from the fit of g_1 data with projected g_1 and Δg data are summarized in Table 4 (the results are rounded off to 1 significant digit). The improved determination of the gluon distribution in the combined fit is also reflected in the reduced uncertainty in α_g, which determines the behavior of Δg at low x. The value obtained from the fit of the g_1 data is $\alpha_g = -0.5 \pm 0.3$. When the projected g_1 and Δg data are considered in the fit we obtain $\alpha_g = -0.5 \pm 0.1$

While the first moment of the polarized gluon distribution can be deduced from scaling violations in g_1, the QCD analysis does not constrain its shape. This can be demonstrated by introducing an additional term into the functional form of the parton distributions,

$$\Delta f(x, Q^2) = N(\alpha_f, \beta_f, a_f)\ \eta_f\ x^{\alpha_f}(1-x)^{\beta_f}(1 + a_f\ x + b_f\ \sqrt{x}), \tag{3}$$

Using this form in the QCD analysis of the g_1 data results in a fit with a node in Δg, that is not allowed by the the more restricted form of Eq. 2. The gluon distribution obtained from a fit with this functional form is shown Fig. 5 where it is also compared with the gluon distribution obtained with the standard form (Eq. 2). The first moment of Δg at $Q^2 = 1$GeV^2 is 0.9 ± 0.3 the same as obtained in the standard fit.

On the other hand, di-jet asymmetries provide good information on the shape of polarized gluon distribution in the measured region. The effect of the additional data on our knowledge of Δg can be demonstrated when the projected values of g_1 and Δg, (obtained from the standard,

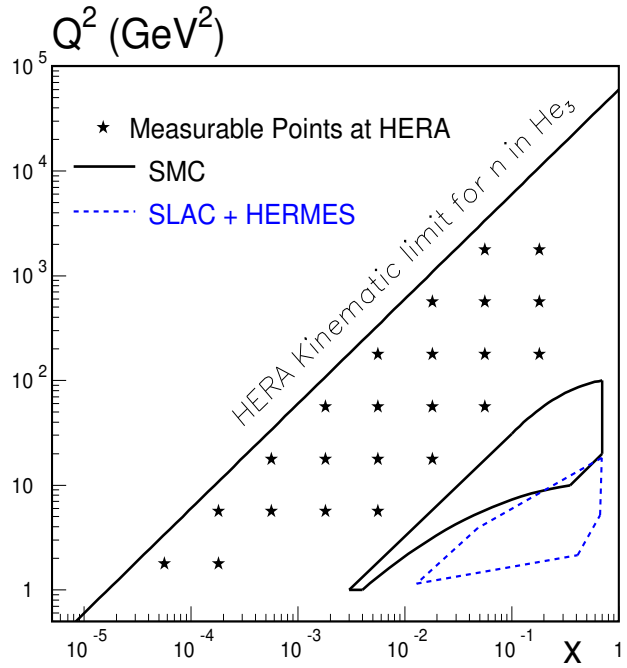

Figure 6: The $x - Q^2$ range available at HERA for g_1^n measurement with polarized ^{3}He beam in comparison with the measured range of other present day experiments.

10 parameter fit) are fitted with 14 parameters, as discussed above. As shown in Fig 5, once the projected data are included in the fit, the polarized gluon distribution obtained from the 14 parameter fit is essentially identical to that obtained from the 10 parameter fit in the region where data from di-jets are introduced. Obviously, Δg remains unconstrained in the high x region where no di-jet data are added and where the Q^2 evolution is small. One may then conclude that the combined analysis will constrain the functional form of the polarized gluon distribution in addition to its first moment.

5 DIS with polarized ^{3}He beam at HERA

We note that future measurements of g_1^n may be possible at HERA if the HERA ring can be injected with doubly charged polarized ^{3}He ions [29]. Acceleration of the $^3He^{+2}$ ions is not expected to pose any fundamental problems in terms of accelerator technology, and may perhaps be considered as a future physics option.

The polarized ^{3}He beam could then be accelerated to 820 GeV, and each nucleon would then have a momentum of $(Z/A) * 820 \sim 550$ GeV. Figure 6 shows the $x - Q^2$ range accessible with such a measurement at HERA in comparison to the present day g_1^n measurements. Deep inelastic scattering events on the neutron could be "tagged" by detecting the remnant proton system along with the scattered electron which avoids the loss in the analyzing power due the dilution factor and brings its value back to 1.0.

Predictions for g_1^n for the HERA kinematic range were calculated using the best fit parton distributions presented in this paper in section 2. Statistical errors were calculated for the

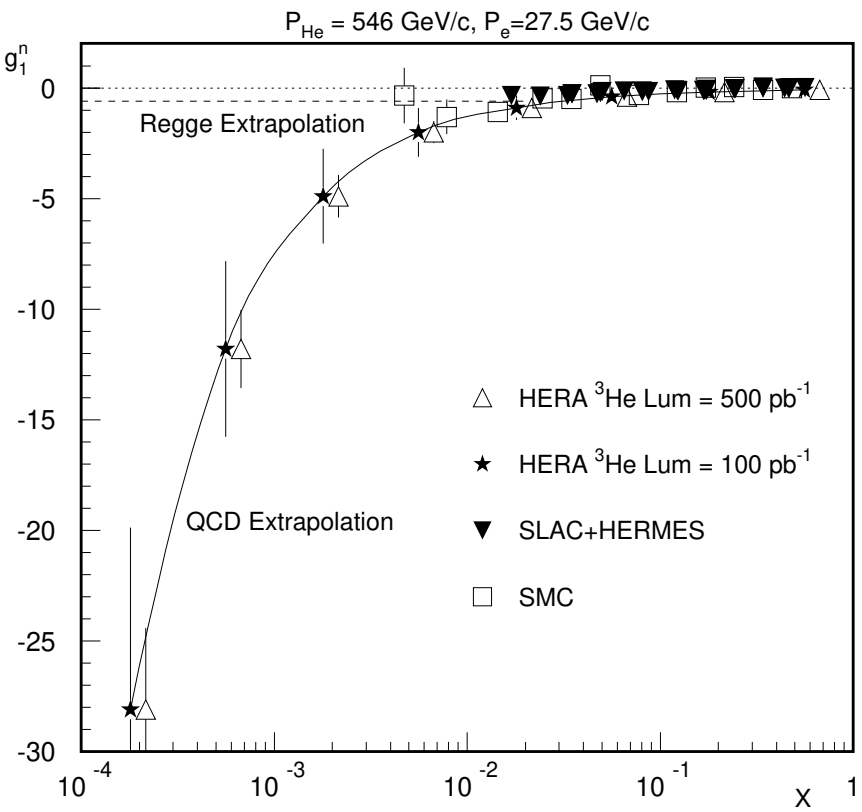

Figure 7: g_1^n vs. x for a possible future measurement with ^{3}He beam is shown. The statistical uncertainty for g_1^n measurement is shown for two different luminosities along with the different possible theoretical scenarios in the low x region which have been considered by present day experiments.

experiments assuming "tagged" experimental measurements, 0.7 polarizations for the ^{3}He and the electron/positron beam, and integrated luminosities of 100 and 500 pb^{-1}. The values of estimated statistical uncertainties are shown in Figure 7 along with the pQCD prediction and the Regge prediction in the low x region, and other present day experimental measurements at higher x values; all at $Q_0^2 = 5$ GeV^2.

It is clear that even with an integrated luminosity of 100 pb^{-1} one would gain important information on the low x behavior of $g_1^{\rm n}$ and be able to distinguish between the present experimentally indistinguishable low x scenarios for the extrapolation into this region. Such measurements along with the measurements on polarized proton will enable direct verification of the Bjorken sum rule to a significantly lower x values compared to the present-day measurements. Furthermore, such measurements would also help reduce the large uncertainties that exist as of today in the pQCD analyses [15, 8, 10].

6 Conclusions

Inclusive DIS measurements at HERA with high integrated luminosity with high energy polarized electrons and polarized protons would yield significant and unique new information on $g_1^{\rm p}(x, Q^2)$ over a much extended range in x and Q^2. For such measurements the false asymmetries should be considerably smaller than the true asymmetries to be measured, and normalization systematic errors should be controlled to be less than 10%. Statistical errors on the points will dominate. The inclusive measurements with HERA discussed in this paper will also provide unique information on the behavior $g_1^{\rm p}(x, Q^2)$ over an unexplored kinematic range, which is of great theoretical interest. In addition we have shown that if polarized ^{3}He can be stored in the HERA ring, equally significant information on the spin structure function of the neutron $g_1^n(x, Q^2)$ can be obtained.

The present uncertainties in the determination of the first moment of the polarized gluon distribution are large. They will be considerably reduced by the pQCD analysis of the g_1 structure function data from HERA. However we have shown that even further reduction in the uncertainty can be achieved if polarized gluon information coming from the di-jet events is used in the analysis in conjunction with the g_1 data.

The fact that HERA is an operating facility with a plan for substantial increase in luminosity and with two major operating detectors, as well as a polarized electron beam, means that only the high energy polarized proton beam needs to be developed. The efforts to achieve that seem well justified and data from such experiments at HERA would provide unique and complementary information to that from other presently proposed experiments.

Acknowledgements: We thank G. Rädel and A. De Roeck for many interesting discussions and information on the di-jet analysis which was used in the combined analysis section of this paper.

References

[1] R. Hofstadter, Rev. Mod. Phys. **28** (1956) 214.

[2] J. Friedman et al., Ann. Rev. Nucl. Science **22**, (1972), 203.

[3] EMC, J. Aubert et al., Phys. Lett. **B123** (1982) 275; NMC, M. Arneodo et al., Phys. Lett. **364** (1995) 107; BCDMS Collaboration, A. C. Benvenuti et al., Phys. Lett. **B223** (1989) 490.

[4] ZEUS Collaboration, M. Derrick et al., Phys. Lett. **B316** (1993) 412;
H1 Collaboration, I. Abi et al., Nucl. Phys. **B407** (1993) 515.

[5] SLAC E80, M. J. Alguard et al., Phys. Rev. Lett. **37** (1976) 1261; ibid **41** (1978) 70;
SLAC E130, G. Baum et al., Phys. Rev. Lett. **51** (1983) 1135;
V. W. Hughes and J. Kuti, Ann. Rev. Nucl. Part. Sci. **33**, (1983) 611.

[6] EMC, J. Ashman et al., Nucl. Phys. **B328** (1989) 1.

[7] SMC, B. Adeva et al., Phys. Lett. **B302** (1993) 533; SMC, D. Adams et al., Phys. Lett. **B329** (1994) 399; SMC, D. Adams et al., Phys. Lett. **B357** (1995) 248; SMC, D.Adams et al., Phys. Lett. **B396** (1997) 338; SMC, D.Adams et al., Phys. Rev. **D56** 9, (1997) 5330.

[8] SM Collaboration, B. Adeva et al., Phys. Lett. **B412** (1997) 414

[9] E143 Collaboration, K. Abe et al., Phys. Rev. Lett. **74** (1995) 346; E143 Collaboration, K. Abe et al., Phys. Rev. Lett **75** (1995) 25;

[10] E154 Collaboration, K. Abe et al., SLAC-PUB-7460 (1997)

[11] G. Altarelli and G. Ridolfi, Nucl. Phys. B Proc. Suppl. **39B** (1995) 106

[12] R. D. Ball, S. Forte and G. Ridolfi, Phys. Lett. **B378** (1996) 255.

[13] M.Glück, E. Reya, M. Stratmann and W. Vogelsang, Phys. Rev. **D53** (1996) 4775 .

[14] T. Gehrmann and W. J. Stirling, Z. Phys. **C65** (1995) 461; Phys. Rev. **D53** (1996) 6100.

[15] Altarelli et al., Nucl. Phys. **B496** (1997) 337.

[16] D. Barber, Polarized Protons in HERA, Proceedings of this workshop; "Acceleration of Polarized Protons to 820 GeV at HERA", SPIN collaboration and DESY Polarization Team, Nov.8, 1996.

[17] R. Ball et al., Proceedings of the Future Physics at HERA Workshop 1995/96, p.777; hep-ph/9609515

[18] "Δg measurements from di-jets", G. Rädel et al., Proceedings of workshop "Future Physics at HERA with polarized protons" DESY (1997).

[19] G. Altarelli and G. Parisi Nucl. Phys. **B126** (1977) 298.

[20] J. Kodaira et al., Phys. Rev. **D20** (1979) 627.

[21] R. Mertig and W.L. van Neerven, Z. Phys. **C70** (1996) 637;
W. Vogelsang, preprint RAL-TR-96-020, hep-ph/9603366 (1996).

[22] HERMES Collaboration, K. Ackerstaff et al., hep-ex/9703005.

[23] R.D. Ball and A. De Roeck, in "DIS96" (World Scientific, 1996), `hep-ph/9609309`

[24] R. L. Heimann, Nucl. Phys. **B64** (1973) 429.

[25] T. Pussieux and R. Windmolders, in "Internal Spin Structure of the Nucleon", V. W. Hughes and C. Cavata, ed.s (World Scientific, Singapore, 1995); also DAPNIA-SPHN-95-10 preprint

[26] N. Akchurin et al., Phys. Rev. **D48** (1993) 3026.

[27] L. Wolfenstein, Ann. Rev. Nuclear Science **6** (1956) 43.

[28] D. Adams et al., Phys. Lett. **B246** (1991) 14.

[29] P. Schüler: Summary of Workshop on High Energy Collider Spin Physics at RHIC and HERA , BNL, August 25,26 1997;
Presentations by Z. Meziani, T. Chupp and M. Ramolis.

[30] E. Leader, Review of the theoretical workshop on proton beam polarimetry, BNL, Proceedings of this workshop.

[31] "Acceleration of Polarized Protons to 120 GeV and 1 TeV at Fermilab", Michigan preprint HE 95-09, (1995).

[32] M. Beddo et al., Proposal for spin physics at RHIC (1993)

[33] C. Y. Prescott et al., Phys. Lett. **B77** (1978) 347; Phys. Lett. **B84** (1979) 524.
V. Yuan et al., Phys. Rev. Lett. **57** (1986) 320 (and references therein);
P. A. Souder et al., Phys. Rev. Lett. **65** (1990) 694.

[34] T. Roser, Nucl. Instr. Meth. **A342** (1994) 343.

[35] R. A. Phelps et al., Phys. Rev. Lett. **72** (1994) 1479.

[36] H1 Collaboration, S. Aid et al., Nucl. Phys. **B445** (1995) 3.